

The completion of the mathematical model by parameter identification for simulating a turbofan engine

Irina Carmen ANDREI^{*1}, Mihai Victor PRICOP¹,
Mihai Leonida NICULESCU¹, Andreea CERNAT¹

*Corresponding author

¹INCAS – National Institute for Aerospace Research “Elie Carafoli”,
Flow Physics Department, Numerical Simulation Unit,
B-dul Iuliu Maniu 220, Bucharest 061126, Romania
andrei.irina@incas.ro*, pricop.victor@incas.ro, niculescu.mihai@incas.ro,
bobonea.andreea@incas.ro

DOI: 10.13111/2066-8201.2015.7.3.3

Received: 28 May 2015 / Received in revised form: 23 June 2015 / Accepted: 23 August 2015
Copyright©2015 Published by INCAS. This is an open access article under the CC BY-NC-ND
license (<http://creativecommons.org/licenses/by-nc-nd/4.0/>)

*3rd International Workshop on Numerical Modelling in Aerospace Sciences, NMAS 2015,
06-07 May 2015, Bucharest, Romania, (held at INCAS, B-dul Iuliu Maniu 220, sector 6)
Section 1 – Launchers propulsion technologies and simulations of rocket engines*

Abstract: *The purpose of this paper is to set up a method to determine the missing engine design parameters (turbine inlet temperature T_{3T} , airflow rate) which significantly influence the jet engines thrust. The authors have introduced a new non-linear equation connecting the fan specific work with the temperature T_{3T} , customized for turbofan. The method of chords, since it converges unconditionally, has been used for solving the non-linear equation of variable temperature T_{3T} . An alternate method, based for the same relation between fan specific work and T_{3T} , has been presented in purpose to determine airflow rate and fan pressure ratio. Two mixed flows turbofans have been considered as study cases. For case #1 it was determined a value comparable to the Turbomeca Larzac turbofan series 04-C6 and 04-C20 which power the AlphaJet machines (series A - Luftwaffe, series E - Dassault Dornier). For the F100-PW229 turbofan, as case #2, being given T_{3T} , then have been determined the airflow rate, fan pressure ratio and fan specific work. After completing the mathematical model with the missing parameters, the performances of the engines at off-design regimes and the operational envelopes revealing i.e. the variations of thrust, specific thrust and fuel specific consumption with altitude and Mach number have been calculated.*

Key Words: *turbofan, engine parameters, performances, off-design regimes, operating maps, numerical simulation*

1. INTRODUCTION

1.1 Justification of the study

In prediction and simulation of jet engine operation, as well as in performance calculation at design and off-design regimes, input data (as engine's and fluid parameters) must be known. Some parameters are given in catalogues or technical specifications of the manufacturers (e.g. Pratt & Whitney [1], Jane's All the World's Aircraft, [2]), while others are not revealed to public access. For most of the cases, there are given the airflow, pressure ratio, by-pass

ratio and the values of the performances (as the thrust and fuel specific consumption) at Sea Level Static SLS take off T/O and cruise conditions. In certain cases, the turbine inlet temperature T3T might be specified, but for many other types of jet engines it is not announced. Other parameters, like pressure losses along the fixed parts of the engine, efficiencies on compression and expansion in turbine respectively are never exposed. Neither the hypothesis regarding the gas as a single fluid or a mixture of species, and/or their properties are specified. For these reasons and to complete the mathematical model of any jet engine, as depicted in Fig. 1, identifying the missing parameters is very important.

The general group of the jet engines, Fig. 1, comprises: a/ the turbojets, b/ turbofans - (b.1/ - with separate flows, for general civil applications; and b.2/ - with mixed flows, for military use), c/ turboprops and d/ turbo-shafts.

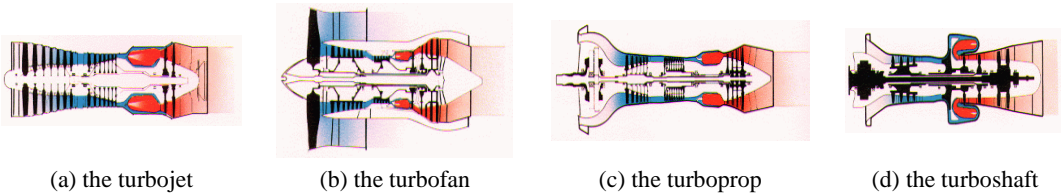


Fig. 1 Types of jet engines, [3-4]

1.2 Goal and prospective

The goal of this paper is to identify a missing parameter that is the turbine inlet temperature T_3^* [K] (also denoted as T3T in international literature, e.g.: Cohen [5], Mattingly [6], Baig [7]) in case of Turbofan # 1 and to determine the airflow rate for the F100-PW229 engine, both constructions being mixed flows turbofans MFTE.

The prospective refers to the numerical simulation of the MFTE, following the completion of its mathematical model. The ultimate purpose is to obtain the operating maps of the engine (depicting the variation of the performances: thrust, specific thrust and specific fuel consumption TSFC, with altitude, flight velocity and engine speed). As a conclusion for the motivation of this study, the completion of the mathematical model and numerical simulation of turbofan engine form the basis for future CFD simulations.

1.3 Some issues on turbofan engines

The main design parameters airflow \dot{M}_a [kg/s] and pressure ratio π_c^* and sometimes the turbine inlet temperature T3T are given in catalogues for most types of jet engines. The bypass ratio K is another design parameter, related only to turbofans, and it is often specified (as in refs. [1-2]). For a large number of turbofan families, the temperature T3T is not announced. Other design parameters (such as pressure losses in air intake and combustor, exit nozzle velocity loss, adiabatic efficiencies on compression and extension, mechanical efficiency) are not exposed. The general approach to determine the missing design parameters is to search combinations and then trim, until a match with the values of the thrust and specific fuel consumption is obtained for take-off and cruise regimes. Following this path means an extremely time-consuming process, sometimes the numerical accuracy is not satisfactory and for certain cases the procedure does not converge. The airflow, pressure ratio and turbine entry temperature T3T, as the main design parameters are focused, since the performances of the engine are highly influenced by them. The influence on the engine performances of the remaining design parameters listed in Table 1 is less in comparison with the main ones. A more efficient approach is the one proposed by the authors, which consists

in the determination of the temperature T3T by using a customized in-house developed method and then the trimming of design parameters expressing losses and efficiencies. The method developed by the authors in order to identify the temperature T3T results from the considerations regarding the mixing the core gas flow (i.e. the mainstream flow) and the bypass flow (i.e. the flow of secondary stream), as illustrated in Fig. 2.a.

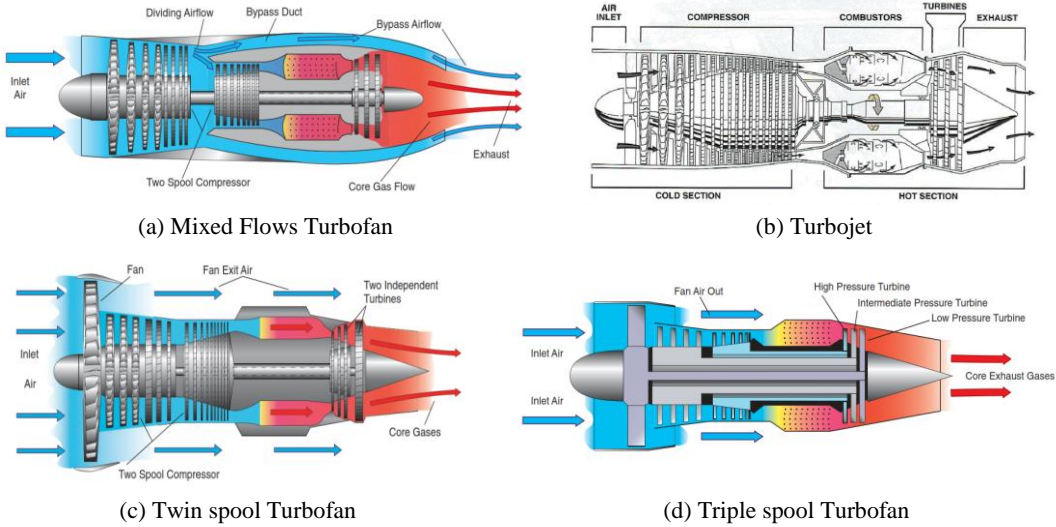


Fig. 2 Schematic diagrams, [3-4]

The reason for referring to the turbojet, Fig. 2.b consists in that it is found as the core engine in the construction of the turbofan, Fig. 2.c and Fig. 2.d, and mixed flows turbofan, Fig. 2.a. The operating equation of the turbofan (1) versus turbojet (2), is also reflecting this aspect; it expresses the work balance, matching the available specific work produced by turbine l_t^* [kJ/kg] and the specific work required for the compression system. In case of turbofans, the compression system comprises both compressor (LPC and HPC) and fan (and therefore there is the specific work of compressor l_c^* [kJ/kg] and the specific work of fan l_v^* [kJ/kg]). In case of turbojets, it is referred only the specific work of compressor l_c^* [kJ/kg]:

$$\eta_m \cdot l_t^* = l_c^* + K \cdot l_v^* \tag{1}$$

$$\eta_m \cdot l_t^* = l_c^* \tag{2}$$

The mechanical efficiency appearing in equations (1) and (2) is correlated (3) with the engine's construction, single spool, twin spool or triple spool:

$$\eta_m = \begin{cases} = 1 & \text{in case of } 1\text{-spool} \\ \in [0.9 - 1.0) & \text{in case of twin / triple - spool} \end{cases} \tag{3}$$

$$K = \frac{\dot{M}_{a2}}{\dot{M}_{a1}} \tag{4}$$

The bypass ratio K (4) defined by the ratio of airflows on secondary versus main streams determines the largest diameter of the turbofan's cross section (Fig. 2.a, c, d) and further has a significant influence on the engine's thrust and aircraft drag.

2. THE STUDY CASES

Threemixed flows turbofan engines (as constructions shown in Fig. 2.a) can be considered as study cases, of which one is manufactured by Honeywell and the other two are the F100-PW220 and F100-PW229 manufactured by Pratt & Whitney. Table 1 details a list of turbofan engine design parameters, as results from a Honeywell Overview [8] and Pratt & Whitney [1] open source.

Tables 2, 3 and 4 contain input data that are required for the performance prediction (at design and off-design regimes), RTO [9], Baig[7] and engine numerical simulation RTO [9], Reed, Turner, Norris and Veres [10].

In order to highlight the specific aspects of the methodology exposed in this paper, this study will focus on two cases: the Turbofan # 1 and F 100-PW 229 engines.

As regards the F100-PW220 engine (a version of which evolved the F 100-PW 229 turbofan engine, although the temperature T3T being not exposed, their values for the two versions are close), the differences between the thrust (i.e. military thrust and thrust with afterburner) are due to the significant modification of overall pressure ratio (meaning additional axial compressor stages) and of bypass ratio (or equivalent airflow rate) in order to increase the thrust.

For these reasons, the focus is on the Turbofan # 1 as test case for determining the temperature T3T and the F100-PW229 engine as test case for calculating the airflow rate.

Table 1 - Main design parameters of the turbofan engines, Honeywell [8], Pratt & Whitney [1]:

Engine reference	Turbofan # 1	F100-PW229	F100-PW220
Manufacturer	Honeywell	Pratt & Whitney	Pratt & Whitney
Overall Pressure Ratio	$\pi_c^* = 22$	$\pi_c^* = 32$	$\pi_c^* = 25$
Fan Pressure Ratio	$\pi_v^* = 1.76$	- not announced	- not announced
Bypass Ratio BPR	$K=2.9$	$K=0.36$	$K=0.63$
Overall Airflow Rate [kg/s]	$\dot{M}_a = 65.772$	- not announced	- not announced
Turbine inlet temperature T3T [K]	- not announced	1623	- not announced
Maximum Thrust F [kN] military thrust // with afterburner	≈ 20.91 // without afterburner	77.5 // 129.7	64.9 // 105.7

Table 2 - The performances of Turbofan # 1, as reference values, [8]:

Conditions // regimes	Net thrust [N]	Fuel specific consumption [kg/Nh]
Thermodynamic, Sea Level, Static SLS, International Standard AtmosphereISA, [10]	20907	0.04650
Takeoff, Sea Level, Static (available to 303 [K])	18905	0.04660
Max Cruise, Mach 0.8 (ISA), 40000[ft] = 12.19 [km]	4493	0.07536

Table 3 - Altitude levels, [8]:

H [ft]	0	10000	20000	30000	40000
H [km]	0	3.048	6.096	9.144	12.192

Table 4 - Mach numbers, [8]:

Mach number at Sea Level Static SLS	0.0
Mach number at Cruise	0.7
Mach number at Max Cruise	0.8

3. MATHEMATICAL SUPPORT

The development of the mathematical support is oriented towards the obtaining the equation and the method for the identification of the turbine inlet temperature T3T, since this parameter has a significant influence upon the performances of the engine.

In case of the mixed flows turbofan presented in Fig. 2.a, the mixing conditions (i.e. either the relations (5) and (6) or both (5) and (7)) that are imposed to the main and secondary streams allow the obtaining for the equation in question.

Technically, the mixing conditions refer to the fact that both streams arrive in the mixing area with equal absolute velocities (5) and either equal static pressures (6) or stagnation pressures (7), Pimsner [11], Rotaru [12], Ciobotea [13], Stanciu [14-15]. The condition of equally stagnation pressures (7) allows in a greater extent the obtaining of minimal pressure losses, rather than the condition of equal static pressures (6), being assumed that the pressure loss coefficients for both streams can be considered equal:

$$C_4 = C_{2v} \tag{5}$$

$$P_4 = P_{2v} \tag{6}$$

$$P_4^* = P_{2v}^* \tag{7}$$

The ratio of turbine inlet versus exit stagnation pressure is defined as the turbine expansion ratio TER δ_t^* (8), which further is expressed by relations (9) and (10), where the specific work of turbine is given by equation (1).

Then, the stagnation pressure at turbine exit p_4^* is expressed (8') as a function of the turbine expansion ratio TER δ_t^* (10) and eventually as function (11) of the stagnation pressure at turbine inlet p_3^* [bar], the specific work of compressor l_c^* (13) and fan l_v^* (14), bypass ratio K and turbine inlet specific enthalpy i_3^* [kJ/kg]. The stagnation pressures at aft fan p_{2v}^* (12) are expressed as a function of the specific work of fan l_v^* (14) and inlet parameters, namely inlet stagnation pressure p_1^* [bar], and inlet stagnation specific enthalpy i_1^* [kJ/kg]:

$$\delta_t^* \equiv \frac{P_3^*}{P_4^*} \tag{8}$$

$$\delta_t^* = \left(1 - \frac{l_t^*}{\eta_t^* \cdot i_3^*} \right)^{-\left(\frac{k'}{k'-1}\right)} \tag{9}$$

$$\delta_t^* = \left(1 - \frac{l_c^* + K \cdot l_v^*}{\eta_m \cdot \eta_t^* \cdot i_3^*} \right)^{-\left(\frac{k'}{k'-1}\right)} \cong \left(1 - \frac{l_c^* + K \cdot l_v^*}{\eta_t^* \cdot i_3^*} \right)^{-\left(\frac{k'}{k'-1}\right)} \tag{10}$$

$$p_4^* \equiv \frac{p_3^*}{\delta_t^*} \quad (8')$$

$$p_4^* = p_3^* \cdot \left(1 - \left(\frac{l_c^* + K \cdot l_v^*}{\eta_t^* \cdot i_3^*} \right) \right)^{\left(\frac{k_g}{k_g - 1} \right)} \quad (11)$$

$$p_{2v}^* = p_1^* \cdot \left(1 + \left(\frac{l_v^* \cdot \eta_v^*}{i_1^*} \right) \right)^{\left(\frac{k}{k-1} \right)} \quad (12)$$

$$l_c^* = i_1^* \cdot \frac{\left((\pi_c^*)^{\left(\frac{k}{k-1} \right)} - 1 \right)}{\eta_c^*} \quad (13)$$

$$l_v^* = i_1^* \cdot \frac{\left((\pi_v^*)^{\left(\frac{k}{k-1} \right)} - 1 \right)}{\eta_v^*} \quad (14)$$

Further, the stagnation pressure at turbine inlet p_3^* is expressed (15) as a function of upstream parameters, being highlighted the combustor pressure loss σ_{ca}^* , compressor pressure ratio π_c^* and inlet stagnation pressure p_1^* .

Likewise, stagnation pressure at fan exit (16) is expressed by the means of the fan pressure ratio π_v^* and inlet stagnation pressure p_1^* :

$$p_3^* = \frac{p_3^*}{p_2^*} \cdot \frac{p_2^*}{p_1^*} \cdot p_1^* = \sigma_{ca}^* \cdot \pi_c^* \cdot p_1^* \quad (15)$$

$$p_{2v}^* = \frac{p_{2v}^*}{p_1^*} \cdot p_1^* = \pi_v^* \cdot p_1^* \quad (16)$$

Eventually, for the stagnation pressure aft turbine p_4^* the relation (17) is obtained:

$$p_4^* = p_1^* \cdot \pi_c^* \cdot \sigma_{ca}^* \cdot \left(1 - \left(\frac{l_c^* + K \cdot l_v^*}{\eta_t^* \cdot i_3^*} \right) \right)^{\left(\frac{k_g}{k_g - 1} \right)} \quad (17)$$

The mixing condition (7) signifying the equality between the stagnation pressure aft turbine p_4^* (17) and stagnation pressure aft fan p_{2v}^* (12), generates a non-linear equation (18) that can be simplified (19), showing that the inlet stagnation pressure p_1^* does not influence at all the turbine inlet temperature T3T:

$$p_1^* \cdot \pi_c^* \cdot \sigma_{ca}^* \cdot \left(1 - \left(\frac{l_c^* + K \cdot l_v^*}{\eta_t^* \cdot i_3^*} \right) \right)^{\left(\frac{k_g}{k_g - 1} \right)} = p_1^* \cdot \left(1 + \left(\frac{l_v^* \cdot \eta_v^*}{i_1^*} \right) \right)^{\left(\frac{k}{k-1} \right)} \quad (18)$$

$$\pi_c^* \cdot \sigma_{ca}^* \cdot \left(1 - \left(\frac{l_c^* + K \cdot l_v^*}{\eta_t^* \cdot i_3^*} \right) \right)^{\left(\frac{k_g}{k_g - 1} \right)} = \left(1 + \left(\frac{l_v^* \cdot \eta_v^*}{i_1^*} \right) \right)^{\left(\frac{k}{k-1} \right)} \quad (19)$$

Further, an equivalent form (20) of relation (19) that allows the calculation of the turbine entry temperature T3T is deduced after applying the function $\ln(x)$. The original contributions provided by the authors are the obtaining of a new relation (20) and the demonstration that its associated algorithm (27) converges faster for obtaining highly accurate numerical solutions.

$$\ln(\pi_c^* \cdot \sigma_{ca}^*) + \left(\frac{k_g}{k_g - 1} \right) \cdot \ln \left(1 - \left(\frac{l_c^* + K \cdot l_v^*}{\eta_t^* \cdot i_3^*} \right) \right) = \left(\frac{k}{k-1} \right) \cdot \ln \left(1 + \left(\frac{l_v^* \cdot \eta_v^*}{i_1^*} \right) \right) \quad (20)$$

Both equations (19) and (20) expressing the turbine inlet temperature T3T can be solved numerically as non-linear equations, with appropriate methods, such as: the method of chords or the method of tangents, Carnahan [16], Spelucci [17], Hjorth-Jensen [18], Berbente [19-20].

4. METHODOLOGY FOR NUMERICAL APPROACH

The method of chords is to be considered for obtaining the numerical solutions with high accuracy and unconditioned convergence (unlike the method of tangents, which is oscillating and does not converge for steepest slopes and requires the modification of the starting point). In order to prepare for the application of the numerical algorithm (27) specific to the method of chords, both equations (19) and (20) can be written of the form (21); therefore, relation (22) is the equivalent form of the equation (19) and relation (23) is the equivalent of (23):

$$f(x) = 0 \quad (21)$$

$$fp(l_v^*) = \pi_c^* \cdot \sigma_{ca}^* \cdot \left(1 - \left(\frac{l_c^* + K \cdot l_v^*}{\eta_t^* \cdot i_3^*} \right) \right)^{\left(\frac{k_g}{k_g - 1} \right)} - \left(1 + \left(\frac{l_v^* \cdot \eta_v^*}{i_1^*} \right) \right)^{\left(\frac{k}{k-1} \right)} \quad (22)$$

$$f(l_v^*) = \ln(\pi_c^* \cdot \sigma_{ca}^*) + \left(\frac{k_g}{k_g - 1} \right) \cdot \ln \left(1 - \left(\frac{l_c^* + K \cdot l_v^*}{\eta_t^* \cdot i_3^*} \right) \right) - \left(\frac{k}{k-1} \right) \cdot \ln \left(1 + \left(\frac{l_v^* \cdot \eta_v^*}{i_1^*} \right) \right) \quad (23)$$

The argument of both functions f (23) and fp (22) is the specific work of fan l_v^* ; the fan pressure ratio π_v^* comes up from equation (24), which was deduced from (14):

$$\pi_v^* = \left(1 + \eta_v^* \cdot \frac{l_v^*}{i_1^*} \right)^{\left(\frac{k-1}{k} \right)} \quad (24)$$

Since there is a single non-linear equation (22) or equivalent (23) with two parameters (the temperature T3T and the specific work of fan l_v^*), the non-determination is off if one parameter is set to a certain reference value (in this case, the temperature T3T) and the other is obtained numerically. Technically, the approach for numerical searching is done according to the next steps, proposed by the authors:

1. Setting the temperature T3T, by considering as reference the values for known similar turbofan constructions, e.g.: T3T [K] = 1175// 1275 Viper 631/633// 1300/ 1375/ 1403 of the Larzac 04-C6 turbofan powering the French trainer version AlphaJet-E, 1433 - for the more powerful Larzac 04-C20 turbofans refitted for the attack version of the Luftwaffe AlphaJet-A machines/ 1800 Eurofighter/ 1850 Rafale, as focused below in Table 5, first column:

Table 5. Solutions of the function $f(23)$ - for large range T3T intervals

$T_3^* [K]$	$l_v^* [kJ/kg]$	π_v^*
1175	34.576	1.4032669
1275	45.644	1.55375834
1300	48.317	1.59175686
1375	56.121	1.70650774
1403	58.955	1.74960491
1433	61.946	1.79591531
1800	95.065	2.3691199
1850	99.135	2.44756941
1900	103.11	2.52597691

2. For a presumed value of the temperature T3T [K], as specified above, there can be set a searching closed interval for the specific work of fan l_v^* , as the argument (25) of the functions (22) and (23), ranging from 20 up to 80 [kJ/kg]; for the values of the T3T temperature higher than 1500 [K], the searching interval can be enlarged, from 20 up to 110 [kJ/kg].
3. The numerical solutions of equations (22) and (23), which represent the specific work of fan l_v^* , are obtained with the algorithm (27) related to the method of chords, Carnahan [16], Spelucci [17], Berbente [19-20]. The calculated values of the specific work of fan as the solutions of the non-linear equation (22) or equivalent (23) are summarized in the second column of Table 5.
4. Once the specific work of fan being determined (with high numerical accuracy, due to the specificity of the method of chords, [16-20], and as shown in Table 6, for a search session, with the presumed T3T = 1300 [K]); then, from relation (24), the fan pressure ratio π_v^* is calculated, see Table 5, the third column.
5. The search is continued until the calculated fan pressure ratio reaches the value specified for the fixed point, which is 1.76:

$$x \equiv l_v^* \quad (25)$$

$$f(x) \equiv f(l_v^*) \quad (26)$$

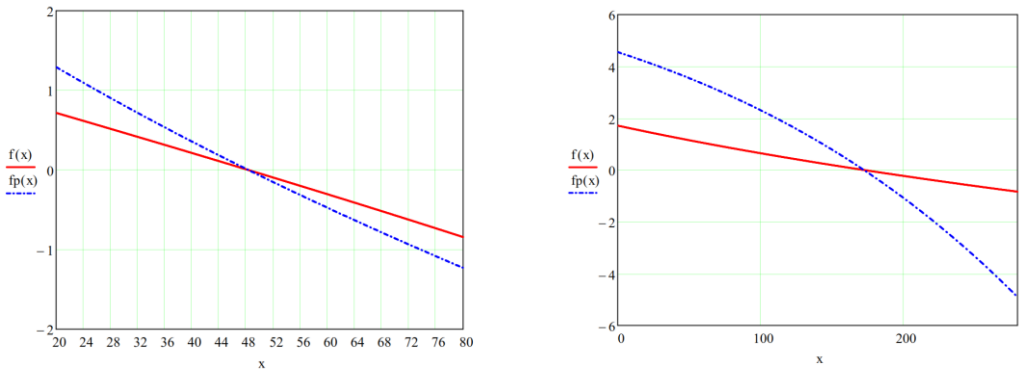
$$x_{n+1} = x_n - (x_n - x_{n-1}) \cdot \frac{f(x_n)}{(f(x_n) - f(x_{n-1}))} \quad (27)$$

$$\begin{cases} x_0 = 20 \\ x_1 = 80 \end{cases} \tag{28}$$

$$n = 1, 2, \dots \tag{29}$$

5. RESULTS AND CONCLUSIONS

The variation of the functions f (23)- in red contours and fp (22)- in blue contours, for both study cases is plotted in Fig. 3. The graphic shown in Fig. 3-a corresponds to the setting of the turbine inlet temperature $T_{3T} = 1300$ [K] with the resulting specific work of fan $l_v^* = 48.31698762$ [kJ/kg] and fan pressure ratio $\pi_v^* = 1.59175686$. For the same T_{3T} setting have been obtained the iterations sequences given by the algorithm (27), for both functions f (23) and fp (22), and exposed below. The non-linear feature of the function f (23) is highlighted much more in Fig. 3-b.



(a) - Case of Turbofan # 1

(b) - Case of F100-PW229 turbofan

Fig. 3 Functions f (23) and fp (22) of argument fan specific work l_v^* [kJ/kg]

Table 6 presents a comparison of the convergence history for functions f (23) versus fp (22), obtained with an in-house developed code for the case of Turbofan # 1. The final results and their convergence history are concluded in Table 8.

Table 6. Convergence history of functions f (23) versus fp (22)

$T_3^* = 1300 [K]$			
$\pi_v^* = 1.76$	$\pi_v^* = 1.59175686$	$\pi_v^* = 1.76$	$\pi_v^* = 1.59175686$
$l_v^* [kJ / kg]$	$f(x)$	$l_v^* [kJ / kg]$	$f(x)$
20	0.71714306	20	1.29241882
80	-0.84352313	80	-1.23120663
47.57065158	0.01926957	47.57065158	0.03138826
48.29492701	5.69915319e-4	48.29492701	9.25957994e-4
48.31700098	-3.4507008e-7	48.31700098	-5.60601596e-7
48.31698762	6.1963213e-12	48.31698762	1.00668363e-11
48.31698762	0	48.31698762	1.55431223e-15
48.31698762	0	48.31698762	0

The solution was obtained with 11 significant digits, which means high accuracy, of order $10^{-(12)}$, after seven iterations when using the function f (23) and after eight iterations for the function fp (22). Therefore, the method of chords converges faster and provides numerical accuracy higher with one order, when using the function f (23).

So far, there can be highlighted some relevant remarks for the methodology and numerical approach:

1. the use of method of chords, since it provides highly accurate solutions and converges unconditioned;
2. the use of the function f (23) rather than the function fp (22), since the results are obtained with less iterations;
3. the two parameters (the temperature T3T and the specific work of fan l_v^*), that appear inside the non-linear equation (23) as well as (22), can be determined numerically, following a step-by-step procedure, as introduced above, which consists in setting a reference value for the temperature T3T and then calculating the specific work of fan as the limit of the convergent sequence (27) and the fan pressure ratio from equation (24).
4. Since the fan pressure ratio at fixed point is 1.76, as given in ref. [8], one can conclude also that the searching interval for the turbine inlet temperature, ranging from 1175 [K] up to 1900 [K], see Table 5, can be significantly narrowed to the range 1403 [K] up to 1433 [K], see Table 7.

The value T3T=1403[K] corresponds to the Larzac 04-C6 turbofan powering the French trainer version AlphaJet-E and T3T=1433[K] is for the more powerful Larzac 04-C20 turbofan refitted for the attack version of the Luftwaffe AlphaJet-A machine.

Table 7. Solutions of the function f (23) - for narrowed range T3T intervals

$T_3^* [K]$	$l_v^* [kJ/kg]$	π_v^*
1403	58.955	1.74960491
1410	59.657	1.760399 \approx 1.76
1433	61.946	1.79591531

In conclusion, there has been determined the value of the turbine inlet temperature T3T = 1410 [K], such that the calculated fan pressure ratio is $1.760399 \approx 1.76$ matches the value specified for the fixed point, which is 1.76, as specified in ref. [8], with the matching value of the specific work of fan being calculated as 59.657 [kJ/kg].

In Table 8 is presented the convergence history for three values of temperature, namely T3T = 1403 [K], 1410 [K] and 1433 [K], corresponding to the narrowed searching interval. The solutions of the non-linear equation (23) of argument $x \equiv l_v^*$ (25) that is the fan specific work, are obtained with 14 significant digits after 7 iterations and after another iteration, the numerical accuracy has been improved with two more orders, i.e. the 16 significant digits have been obtained;

Table 8. Convergence history and final results

$T_3^* = 1403 [K]$		$T_3^* = 1410 [K]$		$T_3^* = 1433 [K]$	
$\pi_v^* = 1.76$	1.74960491	$\pi_v^* = 1.76$	1.760399 \approx 1.76	$\pi_v^* = 1.76$	1.79591531
$l_v^* [kJ/kg]$	$f(x)$	$l_v^* [kJ/kg]$	$f(x)$	$l_v^* [kJ/kg]$	$f(x)$
20	0.9161455	20	0.92829367	20	0.96712693
80	-0.51281138	80	-0.49296558	80	-0.42977795
58.467732	0.01169386	59.188924	0.01117993	61.540134	9.53214253e-3

58.947794	1.76622721e-4	59.65043	1.60274878e-4	61.940676	1.14163633e-4
58.955156	-5.57984042e-8	59.657142	-4.78878279e-8	61.945531	-2.80520026e-8
58.955154	2.65898414e-13	59.65714	2.06057393e-13	61.94553	8.12683254e-14
58.955154	1.44328993e-15	59.65714	0	61.94553	0
58.955154	0	59.65714	0	61.94553	0

Then, after the identification of all missing parameters and the completion of the mathematical model, one can complete the next level, i.e. the determination of performances at design regime and their prediction at off-design regimes, following the methodology described in literature for the mixed flows turbofan, e.g. Cohen [5], Pimsner [11], Rotaru [12], Ciobotea [13], Stanciu [14-15]. Further, the characteristics of the engine parts can be calculated, Stoicescu and Rotaru [21], and optimizations of fan and compressor cascades, Andrei [22], can be carried on.

After these steps, one can proceed to a higher level, which is the numerical simulation of the turbofan engine operation and the calculation of the operating maps of the mixed flow turbofan engine (i.e. the variation of the performances with altitude, velocity and engine speed). All these calculations are based on the properties of working fluids: air, as detailed in ref. [23]- Standard Atmosphere, gas and air-gas mixture.

The graphics shown below have been calculated for the case of Turbofan # 1. In Fig. 4 is plotted the variation with altitude and Mach number of the thrust F [N], in Fig. 5 - the specific thrust F_{sp} [Ns/kg] and in Fig. 6 - fuel specific consumption C_{sp} [kg/Nh].

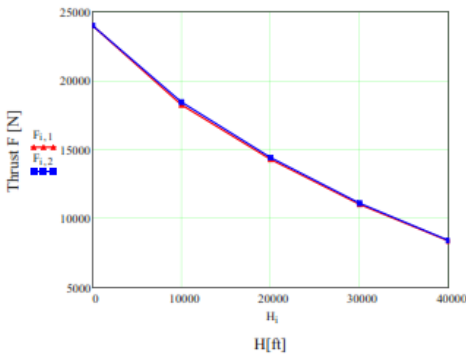


Fig. 4 Variation of engine thrust F [N] with altitude and Mach =0.7 (red contours), Mach = 0.8 (blue contours)

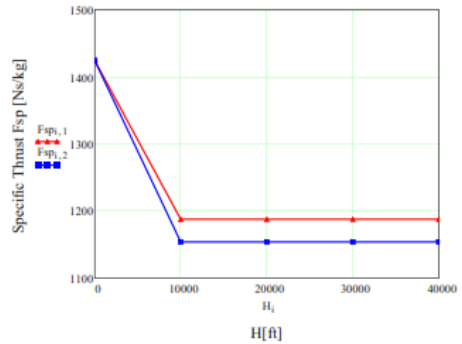


Fig. 5 Variation of specific thrust F_{sp} [Ns/kg] with altitude and Mach =0.7 (red contours), Mach = 0.8 (blue contours)

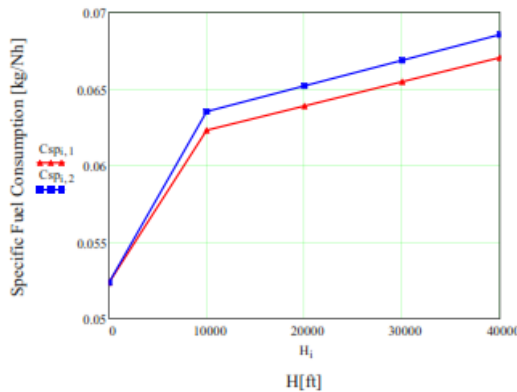


Fig. 6 Variation of specific fuel consumption C_{sp} [kg/Nh] with altitude and Mach =0.7 (red contours), Mach = 0.8 (blue contours)

The conclusions regarding the identification of the missing parameters for the turbofan's mathematical model are presented in Table 9. For study case #1 the temperature $T_{3T} = 1410$ [K] has been identified, while for study case # 2 the fan pressure ratio $\pi_v^* = 4.38$ and the overall airflow rate $\dot{M}_a = 6105.371$ [kg/s] have been identified.

Table 9. Concluding results - Identification of missing parameters

Engine reference	Turbofan # 1	F100-PW229
Overall Pressure Ratio	$\pi_c^* = 22$	$\pi_c^* = 32$
Fan Pressure Ratio	$\pi_v^* = 1.76$	$\pi_v^* = \mathbf{4.38}$
Optimum fan specific work [kJ/kg]	$l_v^* = \mathbf{59.657}$	$l_v^* = \mathbf{172.400}$
Bypass Ratio BPR	$K=2.9$	$K=0.36$
Overall Airflow Rate [kg/s]	$\dot{M}_a = 65.772$	$\dot{M}_a = \mathbf{105.371}$
Turbine inlet temperature T3T [K]	$\mathbf{1410}$	1623
Maximum Thrust F [kN] - military thrust	≈ 20.91	77.5

It has been proven that the numerical solutions of equation (20) can be obtained faster (i.e. with less than 10 iterations), with great precision/accurately, (16 significant digits), and being unconditioned convergence and easy to implement into a home-built code by the means of the method of chords.

Therefore, the authors have developed a simple method for the identification of the missing engine parameters, which provides numerical accuracy. Following the completion of the mathematical model of the MFTE, the simulation of the turbofan engine operation can be done. The graphics shown in Fig. 4, Fig. 5 and Fig. 6 expressing the variation of the engine's performances (thrust, specific thrust and fuel specific consumption) with altitude and flight Mach number conclude the numerical simulation of the MFTE operation.

Therefore, as final remarks, the authors have introduced a new equation (20) that expresses the non-linear dependence of the turbine entry temperature T3T and the fan specific work.

The original approach developed by the authors allowed the completion of the mathematical model of a (mixed flows) turbofan engine, by parameter identification, summarized in Table 9; for the first study case, it was identified the T3T temperature, while for the second study case, there have been identified the airflow rate and fan pressure ratio. The same equation (22) or equivalent (23) was used for parameter identification (as concluded in Table 9, being identified different parameters for each study case).

ACKNOWLEDGEMENT

The study presented in this paper is based on the research activity developed within the INCAS in the frame of the project IAR99-TD.

REFERENCES

- [1] * * * Pratt & Whitney, *Aircraft and Engine Characteristics*, A compilation of data regarding commercial aircraft manufactured by Aircraft Industrie & the Boeing Company (Part 1) and information on commercial and military engines manufactured by Pratt & Whitney, General Electric, International Aero Engines and Rolls Royce (Part2), prepared by Gordon Brown, Marketing Communications and Support, Pratt & Whitney, September 2000.

- [2] * * * *IHS Jane's All the World's Aircraft 2013-2014: Development and Production*, 104th Edition, Susan Bushell (Compiler), David Willis (Compiler), Paul Jackson (Editor), ISBN-13: 978-0710630407, ISBN-10: 07-10630409.
- [3] * * * *The Jet Engine*, Rolls Royce plc, 5th Ed. 1986, Reprinted 1996 with revisions, ISBN 0-902121-2-35.
- [4] * * * *POWERPLANT*, JAA ATPL Training, JEPPESEN, Atlantic Flight Training Ltd, ISBN 0-88487-355-2, JA 310105-000.
- [5] H. Cohen, G. F. C. Rogers, H. I. H. Saravanamuttoo, *Gas Turbine Theory*, 4 ed., Longman, Essex, 1989.
- [6] J. D. Mattingly, *Elements of Propulsion, Gas Turbines and Rockets*, AIAA, Reston, VA, 2006.
- [7] M. F. Baig, H. I. H. Saravanamuttoo, Off-Design Performance Prediction of Single Spool Turbojets Using Gasdynamics, *Journal of Propulsion and Power*, vol. 13, no. 6, pp. 808-810, 1997.
- [8] * * * *TFE-731-40 Overview*, Proven Turbofan Propulsion Technology, HONEYWELL.
- [9] * * * RTO Technical Report 044, RTO-TR-044, AC/323 (AVT-018) TP/ 29, *Performance Prediction and Simulation of Gas Turbine Engine Operation (La prévision des performances et la simulation du fonctionnement des turbomoteurs)*, 2002.
- [10] J. A. Reed, M. G. Turner, A. Norris, J. P. Veres, *Towards an Automated Full-Turbofan Engine Numerical Simulation*, Report NASA/ TM – 2003212494, August 2003, Prepared for the 16th International Symposium on Air-breathing Engines, Cleveland, Ohio, August 31-September 5, 2003.
- [11] V. Pimsner, *Motoare aereactoare*, Ed. Didactica si Pedagogica, Bucuresti, 1983.
- [12] C. Rotaru, *Theory of Turbojet Engines*, Publishing House of Military Technical Academy, Bucharest, 1999.
- [13] V. Ciobotea, *Turboreactorul cu dublu flux*, Ed. Academia Militara, Bucuresti, 1982.
- [14] V. Stanciu, A. Miclescu, G. Mogos, *Aplicatii ale teoriilor sistemelor de propulsie aeriene*, Ed. Printech, Bucuresti, 2005, ISBN 973-718-167-0.
- [15] V. Stanciu, *Bazele propulsiei aeronautice*, Ed. Printech, Bucuresti, 2005, ISBN 978-606-521-894-9.
- [16] B. Carnahan, H. A. Luther, J. O. Wilkes, *Applied Numerical Methods*, John Wiley, New York, 1969.
- [17] P. Spellucci, *Kurz-Skriptur Vorlesung Einführung in die Numerische Mathematik für Maschinenbau MB, Ingenieurwissenschaften WI/MB, VI, Mechanik (BS)*, SS 2003, Technische Universität Darmstadt, <http://numawww.mathematik.tu-darmstadt.de:8081>.
- [18] M. Hjorth-Jensen, *Computational Physics*, University of Oslo, Fall 2007.
- [19] C. Berbente, O. Pleter, S. Berbente, *Numerische Methoden. Theorie und Anwendungen*, Ed. Printech, Bucuresti, 2000.
- [20] C. Berbente, S. Mitran, S. Zancu, *Metode numerice*, Ed. Tehnica, Bucuresti, 1997.
- [21] M. Stoicescu, C. Rotaru, *Turbojet engines. Characteristics and Control Methods*, Publishing House of Military Technical Academy, Bucharest, 1999.
- [22] I. C. Andrei, *Cercetari privind studiul curgerii prin retelele de palete de compresor axial si posibilitati de imbunatatire a performantelor, cu aplicatii la motoarele aereactoare / Andrei N. Irina Carmen.* – Bucuresti : Universitatea Politehnica Bucuresti, Facultatea de Inginerie Aeronautica, 2007. - XXIV, 237 f.: fig.il. color + 1 CD-ROM, Teza de doctorat. Cond. stiintif.: prof. dr. ing. Corneliu Berbente 533.6(043.2), 621.51.001.5(043.2), 621.45(043.2), B-UP 1, Biblioteca U.P.B. inreg. nr. 043/3219.
- [23] * * * *U. S. Standard Atmosphere*, U. S. Government Printing Office, Washington, D. C., Oct. 1976.
- [24] * * * https://en.wikipedia.org/wiki/Pratt_%26_Whitney_F100.